ELSEVIER

Journal of Molecular Graphics and Modelling 20 (2001) 183–197

Journal of Molecular Graphics and Modelling

www.elsevier.com/locate/JMGM

Superimposition-based protocol as a tool for determining bioactive conformations II. Application to the $GABA_A$ receptor

Enrique Gálvez-Ruano [a,*], Isabel Iriepa [a], Antonio Morreale [a], Donald B. Boyd [b]

[a] *Departamento de Química Orgánica, Universidad de Alcalá de Henares, Ctra. Madrid-Barcelona Km. 33,600, Alcalá de Henares, 28871 Madrid, Spain*
[b] *Department of Chemistry, Indiana University-Purdue University at Indianapolis, 402 North Blackford Street, Indianapolis, IN 46202-3274, USA*

Received 19 April 2001; received in revised form 19 June 2001; accepted 19 June 2001

Abstract

The natural templates (NT) superimposition method is used to determine the pharmacophoric requirements of the A subtype of the γ-aminobutyric acid (GABA) receptor. Bioactive conformations for antagonists and agonists are found by superimposing them on a relatively rigid alkaloid bicuculline, which itself is a competitive antagonist at this ligand-gated ion channel receptor. As has been usual in the application of this modeling method, consideration of available experimental data is the cornerstone for obtaining realistic models. The identification of two substructural fragments of bicuculline permitted classification of the ligands. Analysis of the antagonists and agonists with respect to the two substructural fragments revealed two bioactive conformations of the highly flexible GABA molecule, one of which is extended with the nonhydrogenic atoms roughly coplanar torsional angles of −37 and −179° at N–C–C–C and C–C–C–C (carboxyl), respectively. The second bioactive compound is clearly non planar (torsional angles of −81 and −109° at N–C–C–C and C–C–C–C (carboxyl), respectively).

Keywords: Natural template superimposition method; Molecular modeling; GABAergic receptor; Neurotransmitters; γ-Aminobutyric acid; Bioactive conformations

1. Introduction

γ-Aminobutyric acid (GABA (**1**), Fig. 1) acts at the ligand-gated ion channels receptors (LGICR) and is the major inhibitory neurotransmitter in the mammalian central nervous system [1]. Although GABA (**1**) has been known since 1950, it was only after the discovery that many of its actions could be antagonized by bicuculline (**2**, Fig. 1) that it was fully considered a neurotransmitter. A great variety of agonists and antagonists has been prepared which allowed the determination of different GABA receptor subtypes. There are at least three known to date: $GABA_A$, $GABA_B$, and $GABA_C$. The $GABA_A$ subtype, the one in which we are interested here, has been associated with neurological and psychiatric diseases such as epilepsy, Parkinson's, Alzheimer's, and schizophrenia [2–4]. Typical of the LGICR family, the $GABA_A$ receptor is a large transmembrane protein with an overall pentameric structure. The protein consists of several different subunits and bears different binding domains, only one of which is specific for the GABA (**1**) neurotransmitter, and it is the one on which we will focus. The $GABA_A$ domain is sensitive to drugs such as benzodiazepines, steroids, barbiturates, and it is thought that their binding could modify the binding of the GABA (**1**) molecule through allosteric effects. Schematic representations of the $GABA_A$ receptor are shown in [4].

From an experimental point of view, there are three major facts that have been decisive in our understanding of $GABA_A$ receptor function. (1) Extensive mutational analysis performed by Amin and Weiss [5] led to the conclusion that two separated GABA binding domains (BD I and BD II) are crucial for $GABA_A$ receptor activation. It is thought that there are two domains per functional channel. BD I and BD II may interact with a common GABA (**1**) molecule and be part of the same binding site, or BD I and BD II may interact independently with two GABA (**1**) molecules. (2) Wotring and Yoon [6] showed from experimental GABA dose–response curves that the $GABA_A$ channel complex accommodates two agonist molecules in a cooperative way, something also observed by other authors. Moreover, d-tubocurarine (d-tubo (**3**), Fig. 2), a competitive and very rigid antagonist, was shown to block both binding sites. (3)

* Corresponding author. Tel.: +34-91-885-46-05; fax: +34-91-885-46-86.
E-mail address: enrique.galvez@uah.es (E. Gálvez-Ruano).

1093-3263/01/$ – see front matter
PII: S1093-3263(01)00116-4

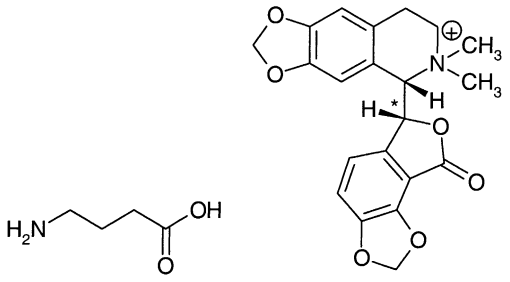

Fig. 1. Chemical diagrams of **1** and **2**. Bicuculline is in the form of the *N*-methylated derivative.

Studies performed by Nielsen et al. [7] on conformationally restricted GABA analogs suggest that these compounds may interact specifically with certain synaptic GABA recognition sites, probably indicating that GABA (**1**) adopts different conformations during its interaction with these sites. In summary, two binding domains seem to exist, and it is plausible that the two GABA (**1**) molecules needed for activation of the channel could have different conformations.

The problem of finding these two specific bioactive conformations becomes apparent when one looks at the GABA (**1**) chemical structure. The existence of three nontrivial rotatable bonds makes it impossible to discern the bioactive conformations when, as in our case, no X-ray structure of the ligand co-crystallized with the receptor is available. Nontrivial rotatable bonds are here defined as those other than to terminal methyl, amino, or hydroxyl groups.

To tackle the problem of finding bioactive conformations in such situations, we have been using relatively rigid alkaloids that act as competitive antagonists for the receptor under study. This technique, which we have called the natural templates (NT) approach [8], has proven useful for generating pharmacophoric models based on bioactive conformations of ligands for several LGICR (5-HT3, nACh, $GABA_A$, and Gly) [9]. With the NT-derived pharmacophoric models in hand, other computational chemistry strategies can be employed. For instance, comparative molecular field analysis (CoMFA), a three-dimensional quantitative structure-activity (3D-QSAR) method, was applied to ligands of the serotonergic receptor (5-HT_3R) [10]. In another example, molecular dynamics simulations were applied to a model of the nAChR binding site [11]. A recent application to the ligands of the glycinergic receptor (GlyR) yielded two pharmacophores, one for agonists and one for antagonists, based on using the structure of strychnine (**4**, Fig. 2) as the NT ([12]; two misprints occurred in Table 3: row 8 gives D-α-AGA, but it should be D-α-ABA; row 9 gives D-α-ABA, but it should be L-α-ABA).

In this paper, we apply the NT protocol to ligands of the $GABA_A$ receptor which share the same binding site as the GABA neurotransmitter. We use bicuculline (**2**) as the 3D template to locate essential features for recognition of $GABA_A$ ligands. Bicuculline (**2**) acts as a competitive antagonist at the $GABA_A$ receptor and at the same binding sites as GABA (**1**) itself [13]. Although it is not the most active antagonist, it is one of the more specific, and it serves as a classical model for competitive antagonists acting at these binding sites. We are able to locate two hypothetical areas in the structure of **2** that serve to classify the ligands studied here. Nonplanar and planar sets of atoms (substructures) in the template are identified, and the different ligands are aligned on these two substructures in a reasonable way. All molecules are subjected to conformational search techniques to assess the energetic accessibility of the proposed bioactive conformations. Experimental results are used as a strict guide in our modeling, allowing us to identify two bioactive conformations for the GABA (**1**) molecule.

Before giving more details on the computational approach undertaken in this paper, it is useful first review the main computational contributions that have been published relative to this field. Also, this introductory review will allow the reader to better appreciate both the differences among these models and the novelty of the way in which we generate bioactive conformations.

Several computational studies have been published on $GABA_A$ ligands relative to the GABA binding site, some of which related specifically to differences between agonist and antagonist behavior based on structural comparisons among the ligands and rigid competitive antagonists as templates. Curtis et al. were the first to compare GABA (**1**) and

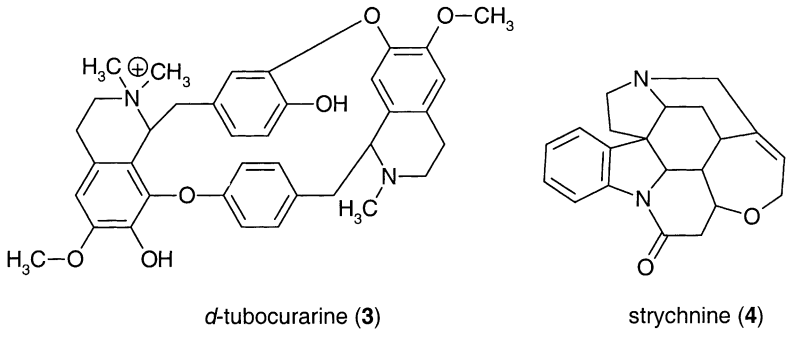

Fig. 2. Chemical diagrams of **3** and **4**.

bicuculline (**2**) from the structural point of view (using hand-held Dreiding models) [14]. Quaternary nitrogen atoms in both molecules and the carboxylic group in GABA (**1**) with the C–C=O lactone moiety in bicuculline (**2**) were associated, giving an extended conformation for GABA (**1**). Since then, molecular modeling studies have focused mainly on the discussion of the anionic part of the interaction: the C–C=O moiety (postulated by Curtis et al. [14]) or the O–C=O moiety (postulated by Steward et al. [15]). These studies afforded a partially folded bioactive conformation for GABA moieties, which seems to be the conformation in agreement with charge calculations [16]. The relative arrangement of the charge centers has also been studied by Pooler and Steward [17] who made a distinction between agonist (with a Y-shaped arrangement and a partially extended conformation for GABA (**1**)) and antagonists (with a linear arrangement and a folded GABA (**1**) conformation).

It has been shown experimentally that the replacement of a 3-isoxazole ring by a 5-isoxazole ring in GABA-related ligands produces an important decrease in their activity and also is able to convert an agonist into an antagonist. Boulanger et al. [18] studied this issue and found that the best system mimicking the localized negative charge distribution occurring at the carboxylic group in GABA (**1**) was the former ring system, whereas a delocalized system, as in the case of the latter, was responsible for lowering or eliminating activity. Pooler and Steward performed a comparison between bicuculline (**2**) and SR95103 (**5**, Fig. 3, antagonists) to study the steric tolerance around the two terminal ends (positive and negative) [19]. The authors concluded that steric congestion is allowed at the positive end and leads to antagonist character, whereas there is no such a problem at the negative end. The importance of the positive end in the binding has been studied with ab initio calculations by Tsuda et al. [20].

In contrast with this assumption, Cioslowski and Fleischmann [21] claimed, based on a molecular similarity analysis using first-order density matrices, that the cationic end in $GABA_A$ agonists does not play any relevant role in the binding, although its relative position with respect to the anionic end could be important. The authors thought that the crucial factor for agonist activity was associated with the negative end. However, their ab initio calculations were based on GABA and only three agonists, all of which were assumed to have planar backbones.

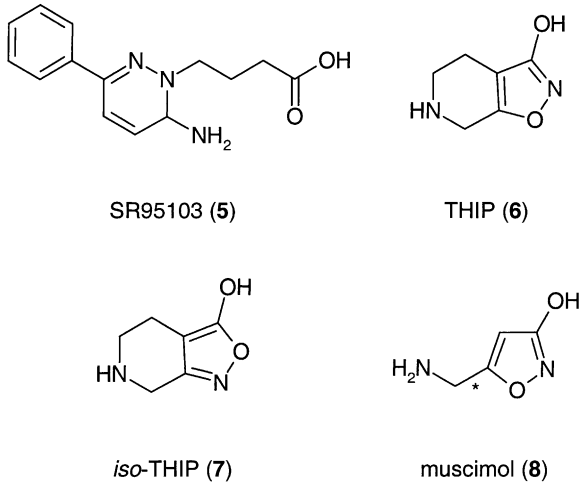

Fig. 3. Chemical diagrams of **5**, **6**, **7**, and **8**.

A QSAR analysis by Lipkowitz et al. [22] on five agonists attempted to correlate steric and electronic descriptors to IC_{50} values. Although no meaningful model was obtained, the relative position between the two ends was found to correlate with the effectiveness of the binding. In particular, more active molecules presented the ammonium center skewed off to one side of a vector that bisects the carboxylate group, whereas the less active ligands had the ammonium group aligned along this vector.

Aprison and Lipkowitz [23] proposed a three-point pharmacophore based on superimpositions between bicuculline (**2**) and some agonists. The negative end of the ligands are located at the O=C–C moiety in bicuculline (**2**). These authors also postulated the existence of a four-point pharmacophore in the antagonist bicuculline (**2**, the remaining oxygen atom in the lactone ring) that could be responsible for the channel blockage. In a more recent contribution [24], it was found that differences between agonists and antagonists could be distinguished by the electrostatic potential energy surfaces using GABA (**1**), THIP (**6**, Fig. 3, agonist) and *iso*-THIP (**7**, Fig. 3, antagonist) as templates. GABA (**1**) and THIP (**6**) presented three clearly defined interaction areas (two negative and one positive), whereas *iso*-THIP (**7**) lost one negative point, making it unable to activate the receptor.

Finally, two pharmacophoric models, one for agonists and one for competitive antagonists, have been reported. In the agonist case, the rigid THIP (**6**) and muscimol (**8**, Fig. 3) structures were used by Lorenzini et al. [25] to define the spatial arrangement of the two centers, with a distance between them of 5.3 Å or greater. In the case of competitive antagonists, Rogman et al. [26] proposed a model in which the aforementioned distance is between 4.6 and 5.2 Å. The latter authors also concluded, in agreement with Ariëns theory [27], that bulky parts in the antagonists ligands could interact with additional binding sites. A new issue noted by Rogman et al. is the ability of a new region not considered before (what we have called the B substructure; see later) in producing hydrogen-bonding interactions with the receptor. This hypothesis was tested through the synthesis of a new compound with enhanced hydrogen bond characteristics in this area yielding the desired results [26].

2. Methodology

Our NT protocol comprises three steps: (1) definition of the natural template. A competitive antagonist (bicuculline (**2**) in this case) is chosen based on its pharmacological profile and its relatively rigid 3D structure. (2) Location of template substructure(s) in fixed conformation(s). Other

competitive antagonists are selected, and steric and electrostatic similarities guided their common superimposition with the template. (3) Confirmation of the substructures. In particular, agonists are fitted to the proposed substructures identified with the antagonists. The pharmacophoric similarity of the antagonists and agonists was thus investigated.

The NT protocol involves repeated passes through the modeling steps to make sure the conformations identified are consistent with all the relevant compounds in the data sets and their receptor specificities. The NT method is superior to looking only for the global energy minimum conformation, which often is not the bioactive conformation of a ligand. Instead, the NT protocol identifies which of the low-energy conformations of the ligands are consistent with a substructure of a large rigid molecule that binds to the receptor of interest. By modeling many ligands, a composite picture of the bioactive conformation can emerge. An implicit assumption of the NT protocol is that proximity of the paired atoms and bonds of the overlapping structures is of primary importance; the relevant substructure of the template need not be the atoms with the most surface exposure.

All the antagonists used here behave as competitive antagonists; in other words, they compete with the agonists for the same binding site. This suggests the plausibility of a common superimposition of both types of ligands. Competitive antagonists, in general, have a more extensive structure that can interact with residues of the protein receptor, in addition to the residues that contact the smaller agonists. This concept is consistent with the Ariëns theory [27] about the difference between antagonists and agonists in general.

2.1. Computational details

All the molecular modeling was done using QUANTA/CHARMm software [28] running on a Silicon Graphics workstation. When available, molecular structures were obtained from published crystallographic studies: bicuculline [29] (**2**), d-tubo [30] (**3**), strychnine [31] (**4**), THIP [22] (**6**; 4,5,6,7-tetrahydroisoxazolo[5,4-*d*]pyridin-3-ol, *iso*-THAZ [32] (**9**; 5,6,7,8-tetrahydro-4*H*-isoxazolo[3,4-*c*]azepin-3-ol), securinine [33] (**10**), pitrazepin [34] (**12**), and isoguvazine [22] (**17**). Structures for muscimol (MUSC, **8**), gabazine (**11**), (*S*)-dihydro-MUSC ((*S*)-DHMUSC (**13**)), *trans*-1-aminocyclopentane-3-carboxylic acid (*t*-ACPA (**14**)), (*R*)-homo-ß-proline (**15**), and (*S*)-3-hydroxy-4-aminobutanoic acid ((*S*)-GABOB (**16**)) were assembled within QUANTA using standard bond lengths and bond angles. All the molecules (agonists and antagonists) were built as protonated species as they exist at physiological pH. Molecules existing predominantly as zwitterions were built in this form.

After assigning atomic charges using the CHARMm Param 23.0 parameter set, molecular mechanics energy minimizations, conformational searches, and molecular dynamics (MD) simulations were done using the CHARMm force field [35]. For the calculations described herein, the dielectric constant of the medium was set to unity, and the cut-off distances for both electrostatic and Lennard–Jones nonbonded interactions were set at 14 Å. The charges of the zwitterions were not explicitly included in the force field calculations other than through the assignment of atom types and force field parameters.

All molecules were energy minimized with the Adopted-Basis Newton–Raphson algorithm. Structures were considered fully optimized when the energy changes between successive iterations were <0.01 kcal/mol. Additional minimizations in the presence of water molecules were performed under the same conditions. A box of TIP3P-type of water molecules 15 Å on a side surrounded each ligand [36]. As we will see later, the inclusion of water molecules is mandatory in some cases because oppositely charged groups inside flexible molecules could be drawn into intramolecular interaction, thereby producing anomalous conformations that cannot be superimposed on the template.

For the more rigid ligands (d-tubo (**3**), strychnine (**4**), THIP (**6**), *iso*-THAZ (**9**), and securinine (**10**)), MD calculations were performed. These ligands lack nontrivial rotatable bonds. A velocity Verlet algorithm was used to integrate Newton's equations of motion using 1 fs time steps. The SHAKE algorithm was used to constrain bond length and bond angles to their equilibrium values with a relative tolerance of 10^{-9} Å. The simulation protocol involved adding kinetic energy to the system for 6 ps, thereby bringing the temperature of the system to 600 K. The system's kinetic and potential energies were allowed to equilibrate for 25 ps. Following this, simulation was carried out at 600 K for 100 ps, during which molecular structures were sampled at 10 ps intervals, yielding 10 structures for post-simulation processing.

For ligands with nontrivial rotatable bonds (bicuculline (**2**), MUSC (**8**), gabazine (**11**), pitrazepin (**12**), (*S*)-DHMUSC (**13**), *t*-ACPA (**14**), (*R*)-homo-ß-proline (**15**), (*S*)-GABOB (**16**), and isoguvazine (**17**)), conformational searches were performed by the systematic search method (grid scan), whereby each torsional angle (marked with asterisks in the figures) is varied over a grid of equally spaced values. Tables 1 and 2 collect the number of torsional angles (NTA), step size for the torsional angles increment (in degrees), and the number of conformations (NC) calculated for each molecule.

It should be clear that the classification of the ligands as rigid or flexible has been made solely in terms of the absence or presence of nontrivial rotatable bonds within the structures. In molecules where these bonds do not exist, MD simulation were performed to explore conformational space. This is an important point especially in those cases as strychnine (**4**) and THIP (**6**), where other conformations for the cyclic moieties should be considered.

2.2. Superimposition protocol

Each ligand (obtained from X-ray data or built with the QUANTA molecular modeling program) was manually

Table 1
Selected results from conformational analysis and superimposition protocol for antagonists

Molecule	NTA	Step size (deg.)	NC	RMS (Å)	d_{N-N} (Å)
Bicuculline (**2**)	1	1	360	–	–
Strychnine (**4**)	MD			0.23	0.45
iso-THAZ (**9**)	MD			0.13	0.06
Securinine (**10**)	MD			0.21	0.36
d-Tubo (**3**)[a]	MD			0.20	0.17
d-Tubo (**3**)[b]				0.17	0.06
Gabazine (**11**)[a]	5	60	7776	0.27	2.83
Gabazine (**11**)[b]				0.18	1.38
Pitrazepin (**12**)[a]	1	1	360	0.08	1.48
Pitrazepin (**12**)[b]				0.25	0.12

[a] Nonplanar superimposition (see text).
[b] Planar superimposition (see text).

Table 2
Selected results from conformational analysis and superimposition protocol for agonists

Molecule	NTA	Step size (deg.)	NC	RMS (Å)	d_{N-N} (Å)
(*S*)-DHMUSC (**13**)	1	1	360	0.35	0.54
t-ACPA (**14**)	1	1	360	0.46	0.28
(*R*)-Homo-ß-proline (**15**)	2	15	576	0.45	0.37
(*S*)-GABOB (**16**)	3	30	1728	0.56	0.40
Isoguvazine (**17**)	1	1	360	0.14	0.06
THIP (**6**)	MD			0.23	0.14
MUSC (**8**)	1	1	360	0.24	0.22

aligned with the template **2** and then flexibly fit to it. The manual alignment considered the congruency of like charges. The subsequent energy minimization superimposition technique acknowledges that molecules are inherently flexible and can change their shapes by rotation around single bonds. The software procedure aligns ligand atoms to template atoms subject to minimizing internal steric and electrostatic energies in the ligand. Atomic coordinates of the alignments are available upon request.

To assess the energetic accessibility of a proposed bioactive conformation, geometry optimizations with and without solvent molecules, conformational searches (for the more flexible ligands), and molecular dynamics (for the more rigid ligands) were performed as detailed in the preceding section. If the difference in energy between a putative bioactive conformation and conformational minima is too great, the likelihood of the existence of that conformation is reduced.

Two quantitative criteria were used for judging the superimposition of the ligands and template. One is the root mean squares (RMS) distance between selected atoms in the ligands and the paired atoms of the template. The selected atoms are the ones marked by the colored chemical symbols in the figures. The second criterion is the distance between the protonated amine nitrogen atom in the ligand and the template. This latter distance is thought to be important because of the role of this heteroatom in receptor recognition and binding. Tables 1 and 2 present the RMS values and the d_{N-N} separations, where the distances were computed after flexibly fitting the molecules.

3. Results and discussion

3.1. $GABA_A$ competitive antagonists

3.1.1. Bicuculline (2) as the natural template

Compared to other NT used in our protocol (strychnine for GlyR, d-tubo for 5-HT_3R, and erysodine for nAChR), it is evident that **2** is not as rigid because it contains one rotatable bond. The 3D structure of **2** has been elucidated by X-ray crystallography [29], and this set of atomic coordinates constitutes an acceptable starting geometry for modeling. In fact, conformational analysis and energy minimization performed in the presence of an aqueous environment, confirm the X-ray structure is close to an energy minimum. Energy minimization of the isolated molecule relaxes the X-ray structure by about 20 kcal/mol, but without appreciable alteration in the conformation (RMS = 0.43 Å). Minimization performed with solvent produces a decrease of 10 kcal/mol with a RMS deviation from the X-ray structure of 0.87 Å. The global minimum obtained from the conformational search is the same minimum found with the simple energy minimization procedure. In light of these RMS values, any of these conformations could be used as template because the main structural features remain close enough and would not

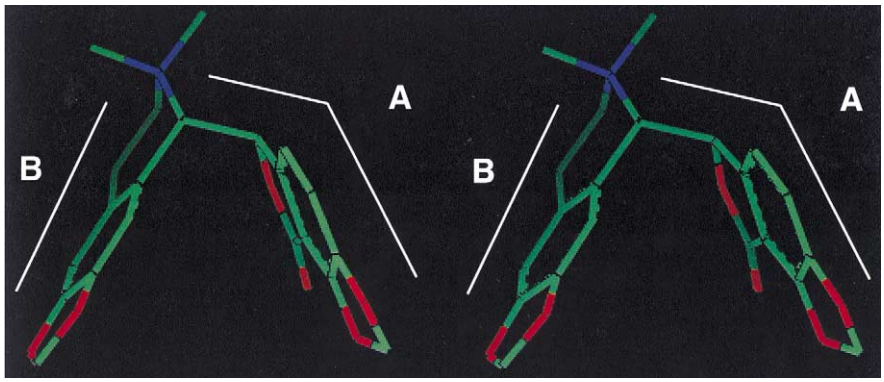

Fig. 4. Stereo view of **2** (bicuculline) showing its A and B substructures used for the alignments. Carbon atoms are colored in green, nitrogen atoms in blue, and oxygen atoms in red. Hydrogen atoms are omitted from the figure for clarity. In this and subsequent stereo figures, the stereo is in the relaxed eye format.

greatly affect in the superimpositions of the different ligands with the template. We use the X-ray atomic coordinates in the modeling described in the remainder of this paper.

Fig. 4 shows a stereo view of bicuculline (**2**) in an orientation to emphasize the two essential structural features ("branches") of our NT. Substructure A is bent creating a nonplanar area. In contrast, substructure B is roughly planar. Whereas it is possible to fit all the ligands to a single substructure of the NT, the RMS values increase significantly. Hence, the use of two substructures is justified. The point is that all the ligands considered here can be classified depending on one or both of these substructures of bicuculline (**2**), as summarized in Table 3.

3.1.2. Nonplanar competitive antagonists: finding the nonplanar bioactive conformation of GABA

Strychnine (**4**, Fig. 2), *iso*-THAZ (**9**, Fig. 5), and securinine (**10**, Fig. 5) are relatively rigid competitive antagonists [32,37,38], which align with the nonplanar substructure of bicuculline (**2**). All three antagonists have been characterized by X-ray crystallography [31–33]. Minimization of **4** and **10** produces an important energy relaxation, but without significant conformational modifications from the X-ray structure. Minimization of **9** yields almost no change in atomic coordinates (RMS = 0.0 Å) or energy (ΔE = 0.02 kcal/mol). A comparison between 13 conformations (X-ray, minimized with and without solvent, and 10 from MD) of **4**, **9**, and **10** yielded low RMS values (0.21, 0.22 and 0.24 Å, respectively), indicating a relative conformational rigidity of these three ligands.

Table 3
$GABA_A$ ligands classified based on the type of superimposition (planar and/or nonplanar) on the bicuculline (**2**) template

Competitive antagonists		Agonists	
Nonplanar	Planar	Nonplanar	Planar
iso-THAZ	d-Tubo	(*S*)-GABOB	Isoguvazine
Strychnine	Gabazine	(*S*)-DHMUSC	THIP
Securinine	Pitrazepin	*t*-ACPA	MUSC
d-Tubo		(*R*)-Homo-ß-proline	
Gabazine			
Pitrazepin			

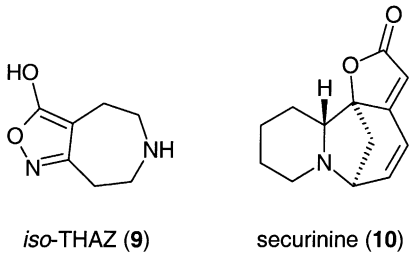

iso-THAZ (**9**) securinine (**10**)

Fig. 5. Chemical diagrams of **9** and **10**.

Fig. 6a shows *iso*-THAZ (**9**) superimposed with bicuculline (**2**). The RMS and $d_{N–N}$ values are 0.13 and 0.06 Å, respectively. The structural and electrostatic (mainly dictated by the quaternary nitrogen atom location) congruency is evident from the figure. The conformer selected for superimposition was the one obtained from the minimization in an aqueous environment; the seven-membered ring is in a chair-like conformation. The gas-phase minimum conformation is 3 kcal/mol below the selected conformation and without appreciable changes from the solvated conformation. Looking at the 10 conformers obtained from the MD simulation, three exhibit a boat-like disposition of the seven-membered ring, and the other seven are chair-like.

Securinine (**10**, RMS = 0.21 Å and $d_{N–N}$ = 0.36 Å, Fig. 6b) can be considered more rigid than *iso*-THAZ in light of the results obtained from MD. The gas-phase minimum energy conformer has an energy 3 kcal/mol above the average value obtained from MD. The conformer from optimization in water, which was the conformation used for superimposing, is 1 kcal/mol below the gas-phase minimum.

Finally, the situation with strychnine (**4**, RMS = 0.23 Å and $d_{N–N}$ = 0.45 Å, Fig. 6c) closely resembles that for compounds **9** and **10**. The energy differences between the

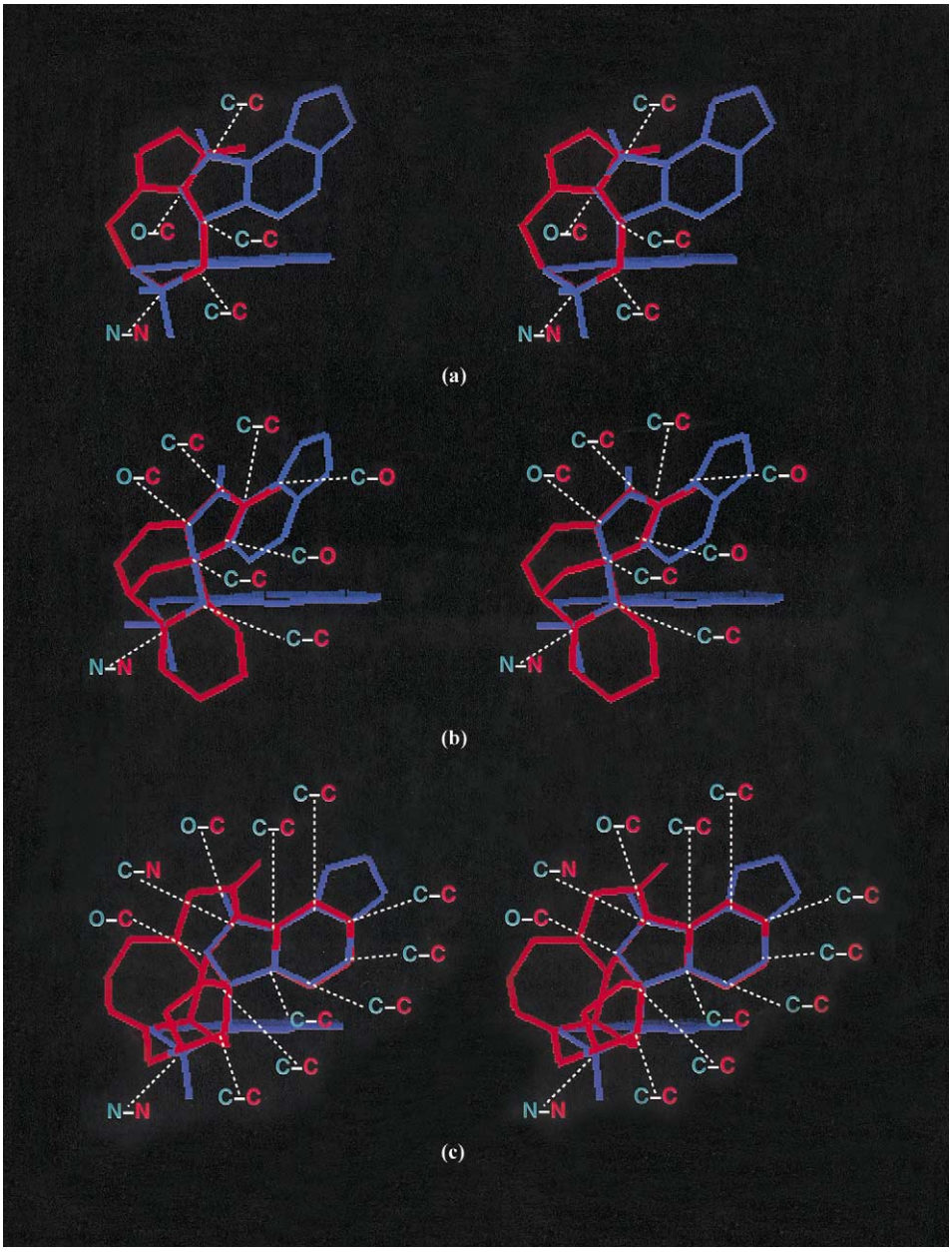

Fig. 6. Stereo view of the alignment of (a) **9** (*iso*-THAZ) and **2**, (b) **10** (securinine) and **2**, and (c) **4** (strychnine) and **2**. In this and subsequent figures showing alignments, the template (**2**) is always in blue, while the superimposed ligand is in red. Labels indicate which pair of atoms is being aligned; the labels are colored the same as the respective molecules. These atom pairs are the ones used to compute the RMS values reported in Tables 1 and 2.

conformers of **4** span only about 4 kcal/mol. Concluding from the RMS values between the different conformers of **4**, **9**, and **10** and their relative energy values, it can be stated that the conformations chosen for superimposition are in all cases highly plausible.

Based on these results, we propose in Fig. 7 the location of the first bioactive conformation of GABA (**1**) aligned on the nonplanar conformation (substructure A) of bicuculline (**2**). The dihedral angles defining this nonplanar conformation of GABA are −81 and −109° at N–C–C–C and C–C–C–C (carboxyl), respectively.

*3.1.3. d-Tubo (**3**), gabazine (**11**), and pitrazepin (**12**): two possible alignments*

The structure of these three ligands can be superimposed in two different ways. One alignment confirms the importance of the nonplanar substructure, whereas the other suggests a second substructure corresponds to a second bioactive conformation for GABA (Table 3).

The most interesting case is d-tubo (**3**, Fig. 2). As mentioned, it has been shown experimentally that this ligand is able to block both $GABA_A$ binding sites [6]. Therefore, there may be two ways of superimposing it on bicuculline

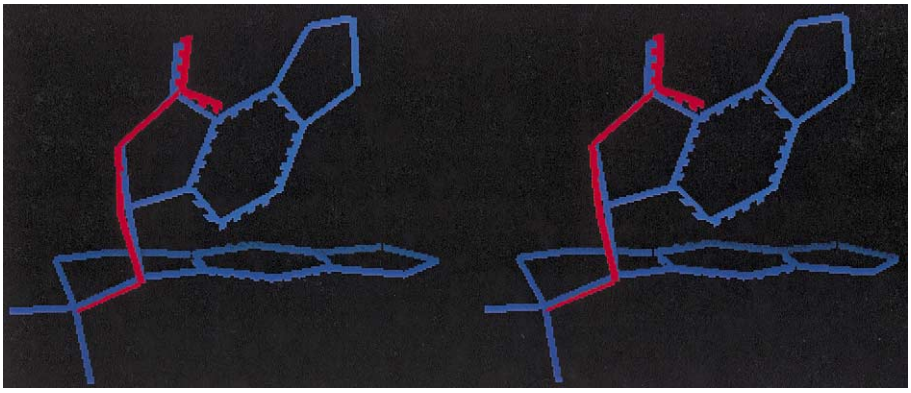

Fig. 7. Stereo view of the alignment of the first bioactive conformation of **1** (in red) with **2** (in blue). The nitrogens of **1** (GABA) and **2** (bicuculline) overlap while a carboxyl oxygen of GABA overlaps with the carbonyl oxygen of the lactone ring of bicuculline. The nonplanar conformation of **1** is aligned with the A "branch" of **2**.

(**2**) (see Fig. 8a–b; part (a) for nonplanar, and part (b) for planar). The values for the RMS and d_{N-N} are 0.20 and 0.17 Å, respectively, for the nonplanar superimposition, and 0.17 and 0.06 Å, respectively, for the planar one. These conformations were geometry optimized (with and without the inclusion of solvent molecules) and subjected to MD. The results show that the 13 conformations (X-ray, minimized with and without solvent, and 10 structures from the MD trajectory) are almost the same, making any of them suitable for our analysis. Some minor structural changes are

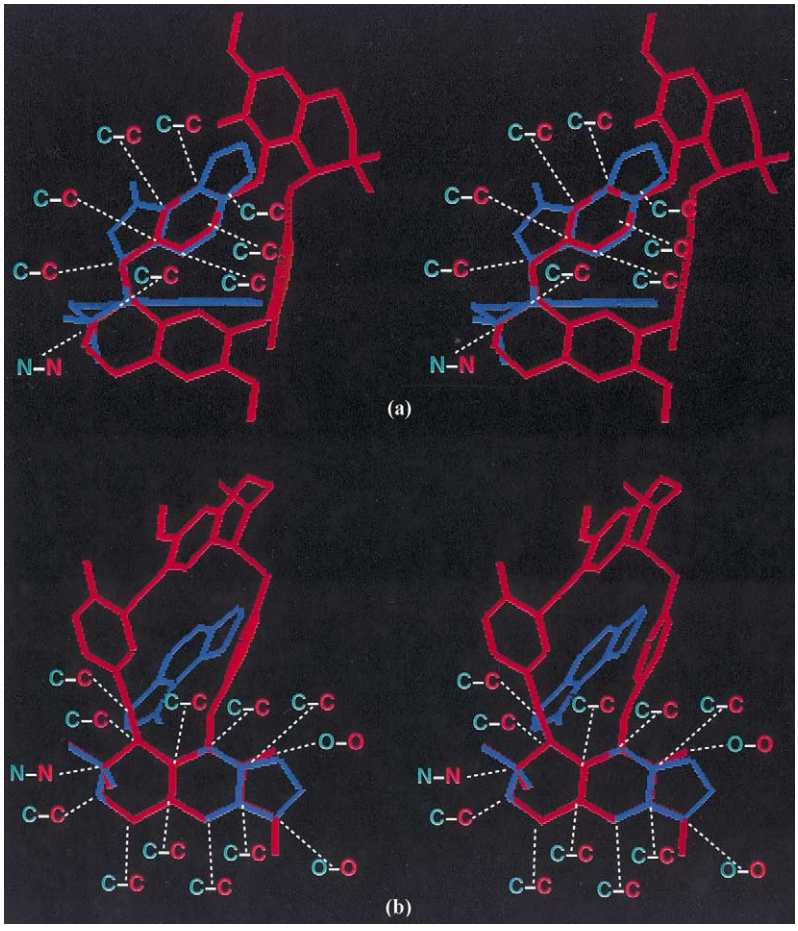

Fig. 8. Stereo view of the alignment of (a) **3** (d-tubo) and **2** (nonplanar substructure) and (b) **3** and **2** (planar substructure).

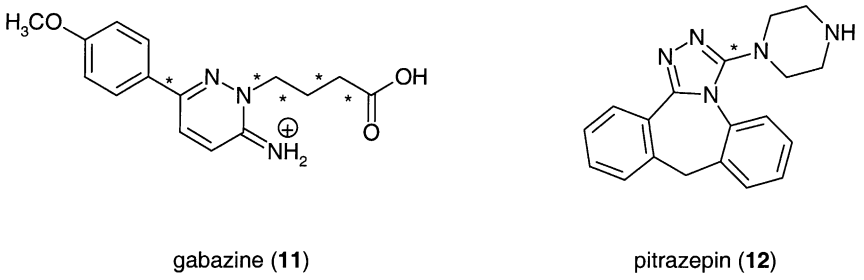

gabazine (**11**) pitrazepin (**12**)

Fig. 9. Chemical diagrams of **11** and **12**.

observed in the middle of the simulation process. The MD trajectory spans a range of 2–3 kcal/mol, and RMS values are between 1.3 and 1.5 Å in the worst case.

A similar situation applies to the other two competitive antagonists: gabazine [39] (**11**, Fig. 9) and pitrazepin [40] (**12**, Fig. 9). Gabazine is a highly flexible molecule having several rotatable bonds, and there is no information about its crystallographic structure. These two issues complicate the elucidation of its bioactive conformation. The conformations used in the superimpositions are shown in Fig. 10a–b (part (a) for the nonplanar and part (b) for the planar). Geometry optimization and conformational analysis (using the five bonds of **11** marked in Fig. 9) yield a conformation in which intramolecular interaction between the carboxylate and $=NH_2^+$ groups exists, but this interaction is not present in Fig. 10a or b. The conformation with the salt bridge in inappropriate for superimposing on bicuculline (**2**). However, when the calculations are performed in an aqueous environment, the superimposable conformations are conserved because the oppositely charged groups are solvated and remain apart. With the superimposable conformations, the values of RMS and $d_{N–N}$ are 0.27 and 2.83 Å for the

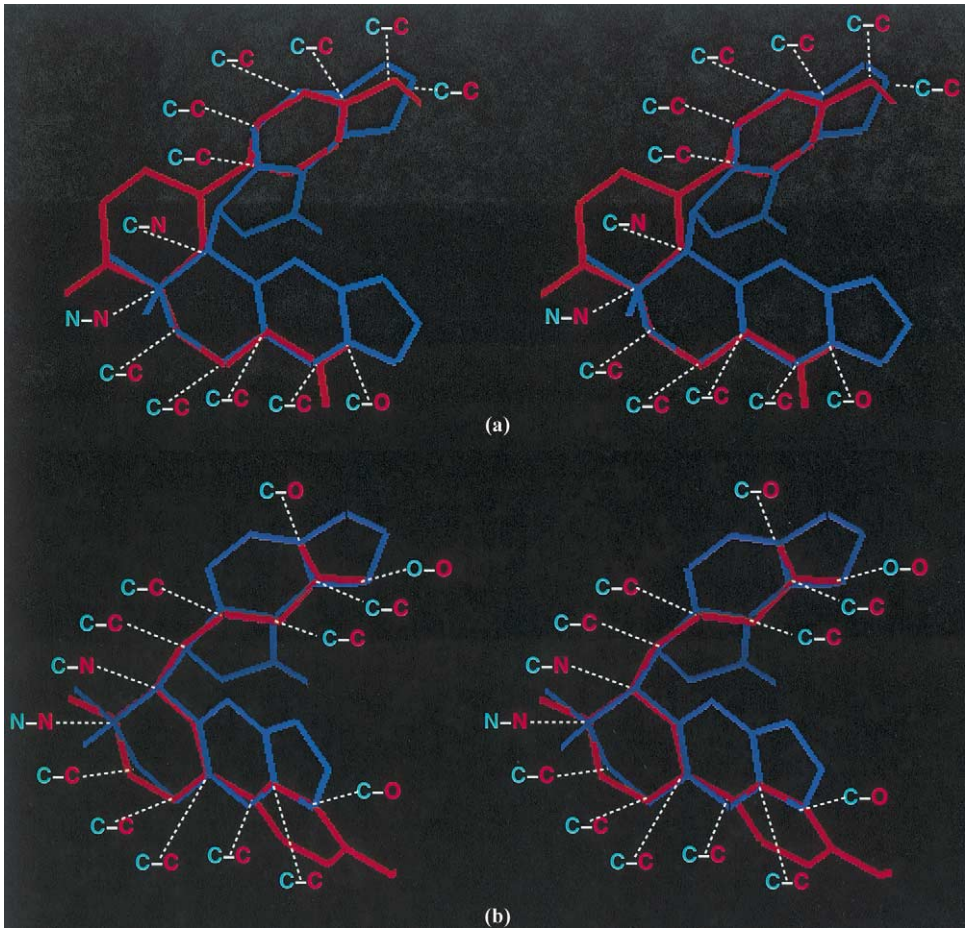

Fig. 10. Stereo view of the alignment of (a) **11** (gabazine) and **2** (nonplanar substructure) and (b) **11** and **2** (planar substructure).

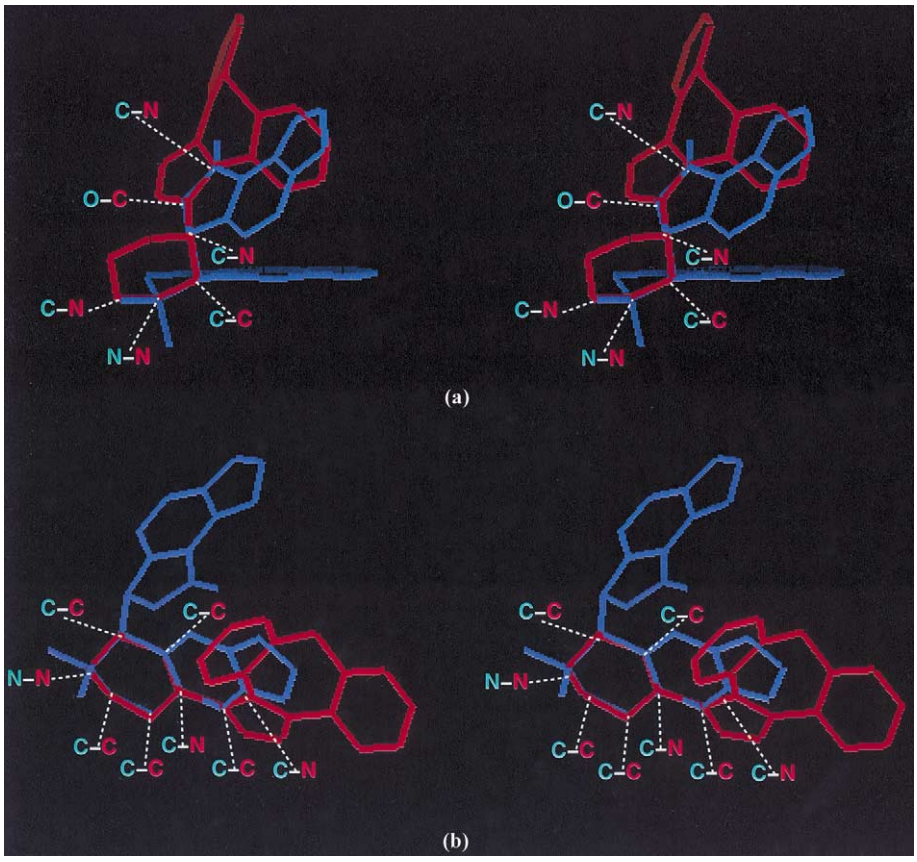

Fig. 11. Stereo view of the alignment of (a) **12** (pitrazepin) and **2** (nonplanar substructure) and (b) **12** and **2** (planar substructure).

nonplanar substructure and 0.18 and 1.38 Å for the planar one, respectively.

Pitrazepin (**12**) has only one rotatable bond, so modeling is easier. Superimposed conformations are shown in Fig. 11a–b (part (a) for nonplanar and part (b) for planar). The optimized geometries (with and without the solvent effect included) and the lowest energy structures from conformational analysis (rotation of the bond in 1° increments) are essentially the same as the proposed one (ΔE = 1–4 kcal/mol and ΔRMS = 0.1–0.4 Å). The values of RMS and $d_{N–N}$ are 0.08 and 1.48 Å for the nonplanar and 0.25 and 0.12 Å for the planar one, respectively.

Generalizing our results (Table 1), the values for RMS and $d_{N–N}$ are mostly better for the planar conformation, but the nonplanar one also seems plausible. Hence, we should consider both. As is the case of d-tubo (**3**), it is possible that gabazine (**11**) and pitrazepin (**12**) each could block both $GABA_A$ binding sites, but this is an issue that remains to be proved by experiments. Based on our analysis, we propose in Fig. 12 the location of a second bioactive

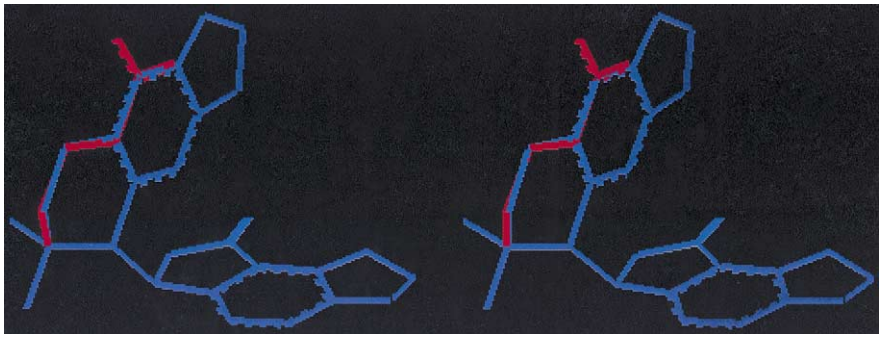

Fig. 12. Stereo view of the alignment of the second bioactive (planar) conformation of **1** (in red) with **2** (in blue). The nitrogens of GABA and bicuculline overlap while GABA's carboxylate is near the dioxolo moiety. The planar conformation of **1** is aligned with the B "branch" of **2**.

conformation of GABA (**1**) aligned with the planar area (substructure B) of bicuculline (**2**). The dihedral angles defining the roughly planar conformation of GABA are −27 and 179° at N–C–C–C and C–C–C–C (carboxyl), respectively.

3.2. $GABA_A$ agonists

There is one interesting issue when comparing agonist structures with the structure of GABA (**1**) itself. All the agonists in one way or another try to mimic a GABA (**1**) bioactive conformation. To do this, some ligands present endocyclic heteroatoms/groups that induce this conformation; in others, the conformation is achieved via intramolecular interactions, as we will see later.

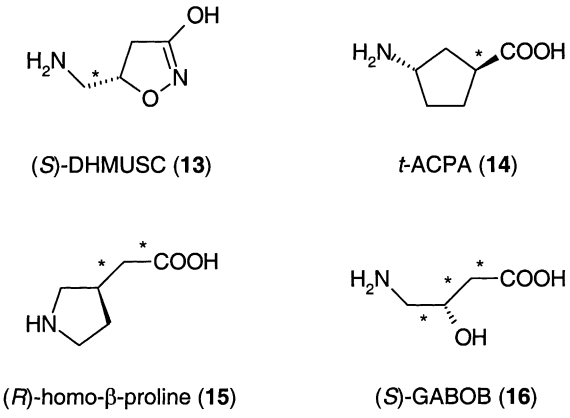

Fig. 13. Chemical diagrams of **13**, **14**, **15**, and **16**.

3.2.1. Nonplanar agonists: confirmation of the nonplanar conformation

(*S*)-DHMUSC (**13**, Fig. 13) is the most potent $GABA_A$ agonist known so far [41]. Fig. 14 shows the proposed bioactive conformation for this ligand superimposed on bicuculline (**2**). The values for RMS and $d_{N–N}$ are 0.35 and 0.54 Å, respectively. Two aspects are important in this conformation. First, the *trans* disposition of $–NH_3^+$ group with respect to the endocyclic oxygen atom, and second, the role played by this oxygen: requiring the conformation to match the nonplanar substructure of bicuculline (**2**). Geometry optimization of this conformation changes it to one in which there is

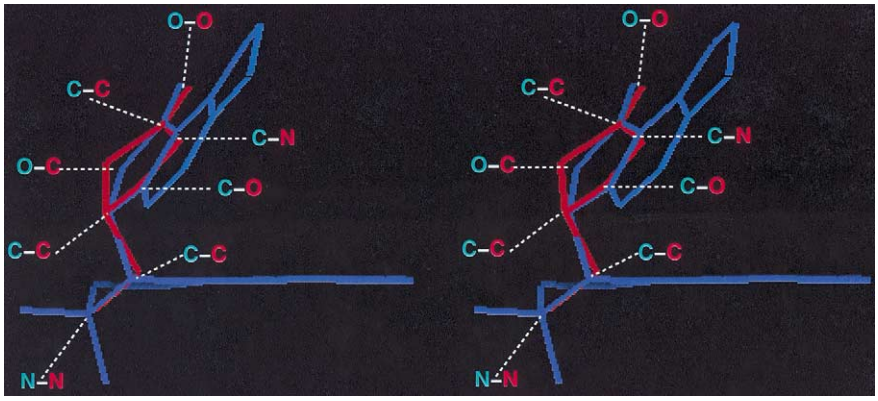

Fig. 14. Stereo view of the alignment of **13** ((*S*)-DHMUSC) and **2**.

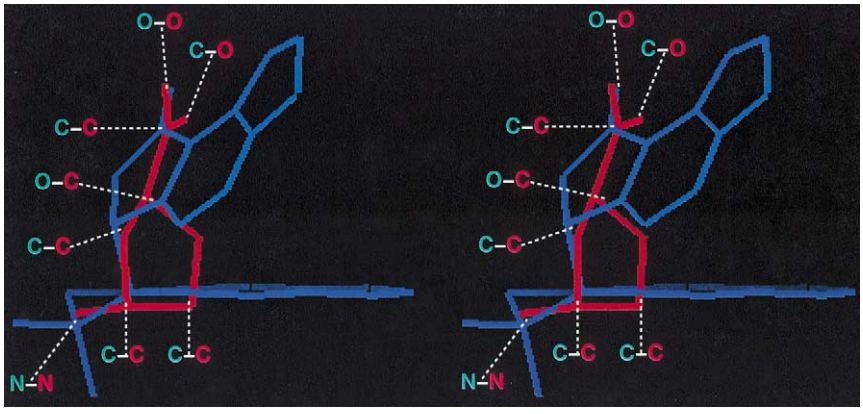

Fig. 15. Stereo view of the alignment of **14** (*t*-ACPA) and **2**.

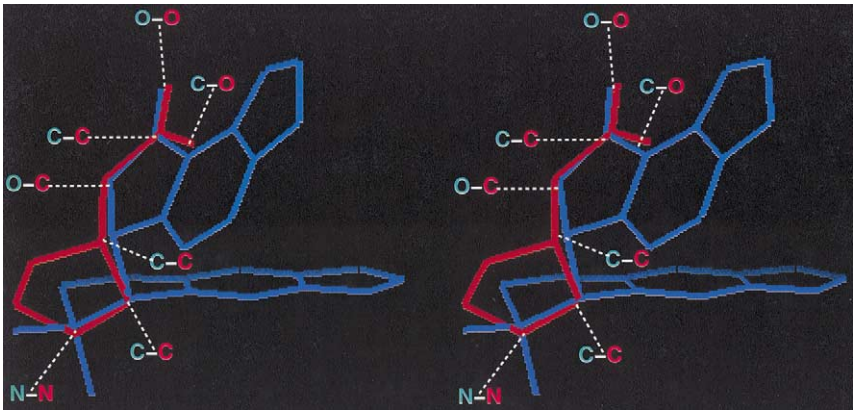

Fig. 16. Stereo view of the alignment of **15** ((*R*)-homo-ß-proline) and **2**.

a stabilizing intramolecular interaction between the $-NH_3^+$ group and the region of the endocyclic nitrogen and oxygen atoms. But this last conformation cannot be fit to the template. Conformational analysis rotating about the C–C exocyclic bond in 1° increments produces the same result. The use of a solvent box yields a conformation that is about 2 kcal/mol more stable than the one proposed for alignment.

A *t*-ACPA [42] (**14**, Fig. 13) possesses an ethylenic bridge, which like the endocyclic oxygen atom in (*S*)-DHMUSC (**13**), forces an appropriate conformation to be adopted. In this case, the values for RMS and d_{N-N} are 0.46 and 0.28 Å, respectively, for the proposed conformation shown in Fig. 15. Geometry optimization (with and without solvent) and conformational analysis (1° increments in the exocyclic C–C bond) of **14** yield almost the same conformation with energy differences of 2–3 kcal/mol among them.

(*R*)-Homo-ß-proline [7] (**15**, Fig. 13) also possesses an ethylenic bridge which restricts its conformation. The values for RMS and d_{N-N} are 0.45 and 0.37 Å, respectively, for the proposed conformation shown in Fig. 16. As in the case of (*S*)-DHMUSC (**13**), the proposed bioactive conformation is not the same as the minimum energy ones obtained from optimization or from a conformational search (rotating the two possible bonds in 15° increments). However, performing the optimization in the presence of water molecules yields a conformation suitable for superimposing, and hence, this conformation is viewed as the bioactive one.

The nonplanar agonist (*S*)-GABOB [41] (**16**, Fig. 13) maintains the appropriate conformation through intramolecular interaction between the hydroxyl hydrogen atom and one of the carboxylic oxygen atoms. This interaction forms a five-membered pseudo cycle in the same spatial disposition as the one in (*S*)-DHMUSC (**13**). Fig. 17 shows the superimposition of **16** with bicuculline (**2**), affording values for the RMS and d_{N-N} of 0.56 and 0.40 Å, respectively. On the other hand, the optimized conformation is folded with the carboxylate and $-NH_3^+$ groups interacting. Although this conformation represents the global minimum (all of the C–C bond were rotated in 30° increments), it cannot be superimposed with bicuculline (**2**) in a satisfactory way. Again, the inclusion of water molecules preserves the desired conformation.

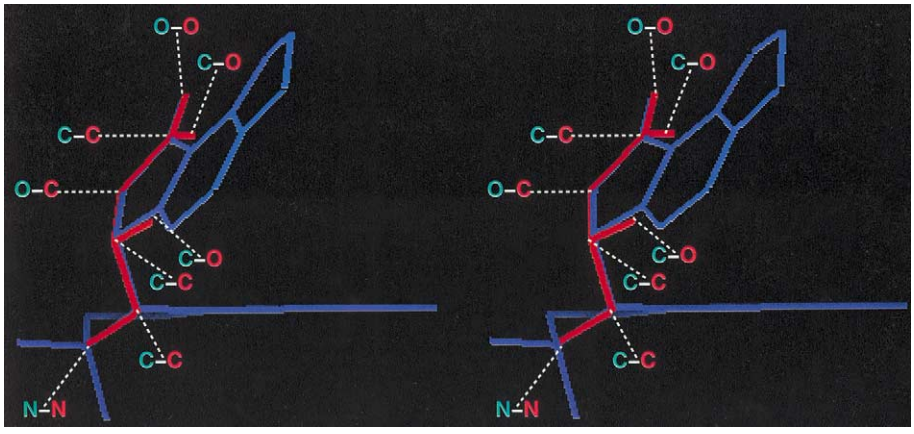

Fig. 17. Stereo view of the alignment of **16** ((*S*)-GABOB) and **2**.

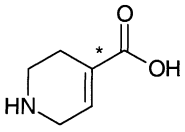

isoguvazine (**17**)

Fig. 18. Chemical diagram of **17**.

3.2.2. Planar agonists: confirmation of the planar conformation

The modeling for one of these, isoguvazine [43] (**17**, Fig. 18), is displayed in Fig. 19 superimposed with bicuculline (**2**). The RMS and d_{N-N} values are 0.14 and 0.06 Å, respectively. In this case, the superimposed conformation, as well as the ones from optimization in vacuum and in water, and the global minimum one obtained from conformational search (rotating the exocyclic C–C bond in 1° increments) are essentially the same, both structurally and energetically (maximum energy difference 1.5 kcal/mol).

THIP [43] (**6**, Fig. 3) is more rigid than the previously mentioned agonists, but presents similar behavior. Comparison of the 13 structures (superimposed, minimized with and without water, and 10 from the MD trajectory) revealed no notable differences in the structure or energy. The values for the RMS and d_{N-N} are 0.23 and 0.14 Å, respectively. The superimposition is shown in Fig. 20.

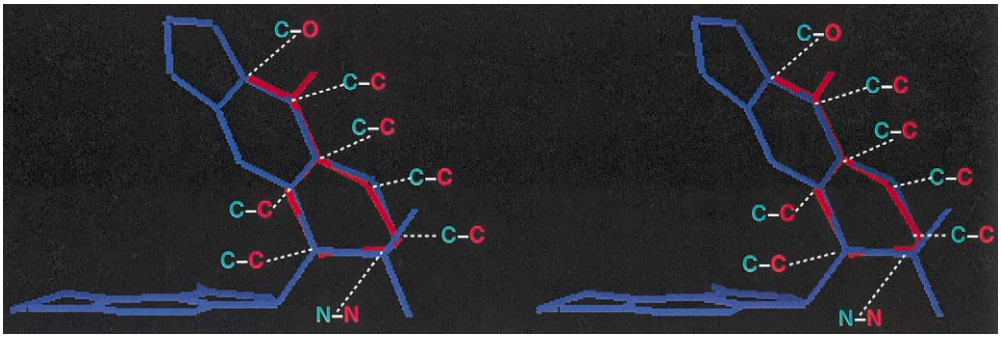

Fig. 19. Stereo view of the alignment of **17** (isoguvazine) and **2**.

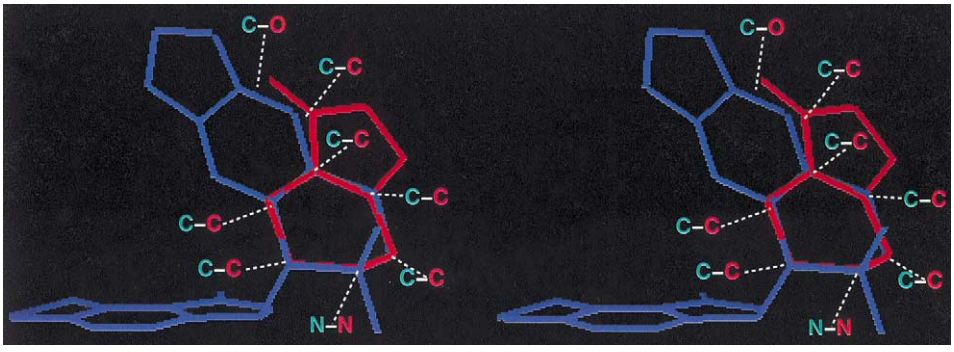

Fig. 20. Stereo view of the alignment of **6** (THIP) and **2**.

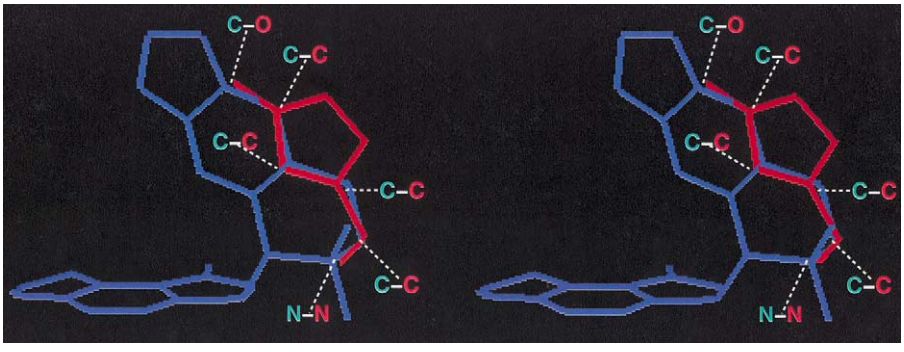

Fig. 21. Stereo view of the alignment of **8** (MUSC) and **2**.

The last ligand we consider is MUSC [44] (**8**, Fig. 3). The proposed bioactive conformation displays a *trans* configuration for the $-NH_3^+$ group in relation with the endocyclic oxygen atom. The minimum energy conformation agrees well with this disposition, but the global minimum and the minimum obtained with solvent molecules tend to be in the *cis* configuration. The superimposed conformation, shown in Fig. 21, is only 1 kcal/mol higher in energy than the minimum in water. The values for the RMS and d_{N-N} are 0.24 and 0.22 Å, respectively.

4. Concluding remarks

It is important to note, as mentioned in the introduction, that previously reported molecular modeling studies of $GABA_A$ ligands focused on looking for either one bioactive conformation or two when comparing agonists and antagonists. In the latter comparison [26], the competitive behavior of the antagonists was not taken into account by previous authors. Whereas previous authors looked for differences between antagonists and agonists, we looked for 3D similarities.

The advance in the present paper is that we were able to propose two bioactive conformations of GABA that can be used simultaneously for agonists and antagonists. The ligands, either agonists or antagonists, were divided into planar and nonplanar classes depending on their superimposition on two substructures of bicuculline, taken as the natural template.

At one end of the chain of atoms in the $GABA_A$ ligands is a protonatable nitrogen, which produces a positive electrostatic field. At the other end of the chain are one or more oxygen atoms which produce a negative electrostatic field. The ligands and GABA itself show a congruency in their charge distributions in the alignments we propose. The domains of the $GABA_A$ receptor are expected to produce complementary electrostatic fields. The competitive antagonists are in general larger molecules than the agonists and, therefore, would occupy more of the receptor's volume.

The energetic accessibility of the proposed bioactive conformations was investigated via molecular mechanics geometry optimizations and conformational searches for the more flexible molecules (with rotatable bonds affecting gross conformation) and molecular dynamics for the more rigid structures (without these bonds). Such calculations performed in vacuum were sometimes unable to reveal the bioactive conformations; inclusion of explicit solvent (water) molecules is mandatory for obtaining satisfactory results in those cases. In all cases studied here, the bioactive conformations were within a few kilocalories per mole of the lowest energy conformations.

Using the models we have reported here, more sophisticated techniques can be employed in the future. For instance, families of related compounds could be aligned for 3D-QSAR studies.

References

[1] D.R. Curtis, G.A.R. Johnston, Amino acids transmitters in the mammalian central nervous system, Ergebn. Physiol. 69 (1974) 97–188.
[2] D.I.B. Kerr, J. Ong, $GABA_A$ agonists and antagonists, Med. Res. Rev. 12 (1992) 593–636.
[3] P. Krogsgaard-Larsen, B. Frolund, F.S. Jorgensen, A. Schousboe, $GABA_A$ receptor agonists, partial agonists, and antagonists. Design and therapeutic prospects, J. Med. Chem. 37 (1994) 2489–2505.
[4] P. Krogsgaard-Larsen, B. Frolund, U. Kristiansen, K. Frydenvang, B. Ebert, $GABA_A$ and $GABA_B$ receptor agonists, partial agonists, antagonists and modulators: design and therapeutic prospects, Eur. J. Pharm. Sci. 5 (1997) 355–384.
[5] J. Amin, D.S. Weiss, $GABA_A$ receptor needs two homologous domains of the ß-subunit for activation by GABA but not by pentobarbital, Nature 266 (1993) 565–569.
[6] V.E. Wotring, K.-W. Yoon, The inhibitory effects of nicotinic antagonists on currents elicited by GABA in rat hippocampal neurons, Neuroscience 67 (1995) 293–300.
[7] L. Nielsen, L. Brehm, P. Krogsgaard-Larsen, GABA agonists and uptake inhibitors. Synthesis, absolute stereochemistry, and enantioselectivity of (*R*)-(−)- and (*S*)-(+)-homo-ß-proline, J. Med. Chem. 33 (1990) 71–77.
[8] E. Gálvez-Ruano, I. Iriepa, A. Morreale, Natural templates for nervous system receptor ligands. Competitive antagonist alkaloids at the glycinergic, GABAergic, cholinergic and serotoninergic receptors, in: R.A. Abramovitch, A. Brossi, J.P. Kutney, S. Oae, S.W. Pelletier, C. Szantay, M. Tisler (Eds.), Trends in Heterocyclic Chemistry, Research Trends, Trivandrum, India, 1997, pp. 135–144.
[9] M.H. Aprison, E. Gálvez-Ruano, K.B. Lipkowitz, Comparative binding mechanisms at cholinergic, serotonergic, glycinergic and GABAergic receptors, J. Neurosci. Res. 43 (1996) 127–136.
[10] A. Morreale, E. Gálvez-Ruano, I. Iriepa-Canalda, D.B. Boyd, Arylpiperazines with serotonin-3 antagonist activity: a comparative molecular field analysis, J. Med. Chem. 41 (1998) 2029–2039.
[11] E. Gálvez-Ruano, I. Iriepa-Canalda, A. Morreale, K.B. Lipkowitz, A computational model of the nicotinic acetylcholine binding site, J. Comput.-Aided Mol. Des. 13 (1999) 57–68.
[12] E. Gálvez-Ruano, I. Iriepa, A. Morreale, D.B. Boyd, Superimposition-based protocol as a tool for determining biactive conformations. I. Application to ligands of the glycinergic receptor (GlyR), J. Mol. Graphics Modell. 19 (2001) 331–337.
[13] L.M. Nowak, A.B. Young, R.L. MacDonald, GABA and bicuculline actions on mouse spinal cord and cortical neurons in cell culture, Brain Res. 244 (1992) 155–164.
[14] D.R. Curtis, A.W. Duggan, D. Felix, G.A.R. Johnston, GABA, bicuculline and central inhibition, Nature 226 (1970) 1222–1224.
[15] E.G. Steward, R. Player, J.P. Quilliam, D.A. Brown, M.J. Pringle, Molecular conformation of GABA, Nat. New Biol. 233 (1971) 87–88.
[16] E.G. Steward, P.W. Borthwick, G.R. Clarke, D. Warner, Agonism and antagonism of γ-aminobutyric acid, Nature 256 (1975) 600–602.
[17] G.W. Pooler, E.G. Steward, Structural comparisons between GABA, bicuculline and semi-rigid GABA analogues, J. Mol. Struct. 156 (1987) 247–253.
[18] T. Boulanger, D.P. Vercauteren, F. Durant, J.-M. Andre, 3- and 5-isoxazolol zwitterions: an ab initio molecular orbital study relating to GABA agonism and antagonism, J. Theor. Biol. 127 (1987) 479–489.
[19] G.W. Pooler, E.G. Steward, Structural factors governing agonist and antagonist activity in the $GABA_A$ system, Biochem. Pharmacol. 37 (1988) 943–945.
[20] M. Tsuda, T. Takada, M. Mizayaki, Y. Uda, S. Kuzuhara, K. Kitaura, A study of GABA and its analogues using the molecular orbital method, J. Mol. Struct. 280 (1993) 261–272.

[21] J. Cioslowski, E.D. Fleischmann, Ab initio electronic structure calculations of molecular similarity: a case study of 4-aminobutyric acid and its agonists, Croatica Chem. Acta 66 (1993) 113–121.
[22] K.B. Lipkowitz, R.D. Gilardi, M.H. Aprison, Electronic and structural features of γ-aminobutyric acid (GABA) and four of its direct agonists, J. Mol. Struct. 195 (1989) 65–77.
[23] M.H. Aprison, K.B. Lipkowitz, On the $GABA_A$ receptor: a molecular modelling aproach, J. Neurosci. Res. 23 (1989) 129–135.
[24] E. Gálvez-Ruano, M.H. Aprison, D.H. Robertson, K.B. Lipkowitz, Identifying agonistic and antagonistic mechanisms operative at the GABA receptor, J. Neurosci. Res. 42 (1995) 666–673.
[25] M.L. Lorenzini, L. Bruno-Blanch, G.L. Estiú, Structural and electronic factors associated with the activity in the $GABA_A$ system, J. Mol. Struct. (Theochem) 454 (1998) 1–16.
[26] D. Rogman, T. Boulanger, R. Hoffmann, D.P. Vercauteren, J.-M. Andre, F. Durant, C.-G. Wermuth, Structure and molecular modelling of $GABA_A$ receptor antagonists, J. Med. Chem. 35 (1992) 1969–1977.
[27] E.J. Ariëns, A.J. Beld, J.F. Rodrigues de Miranda, A.M. Simonis, The pharmacon–receptor–effector concept: a basis for the understanding the transmission of information in biological systems, in: R.D. O'Brien (Ed.), The Receptors, Vol. 1, Plenum Press, New York, 1979, pp. 33–91.
[28] Molecular Simulations Inc. (now Accelrys), San Diego, CA, www.msi.com, www.accelrys.com.
[29] K.B. Lipkowitz, R.D. Gilardi, M.H. Aprison, Molecular mechanics and X-ray crystallographic analysis of bicuculline salt conformations, J. Mol. Struct. 178 (1988) 305–313.
[30] P.W. Codding, M.N.G. James, The crystal and molecular structure of a potent neuromuscular blocking agent: d-tubocurarine dichloride pentahydrate, Acta Crystallogr. Sect. B 29 (1973) 935–942.
[31] A. Mostad, Structural study of the strychnine molecule in crystals of the free base and of the nitric acid complex, Acta Chem. Scand. Ser. B 39 (1985) 705–716.
[32] L. Brehm, P. Krogsgaard-Larsen, K. Scaumburg, J.S. Johansen, E. Falch, D.R. Curtis, Glycine antagonists. Synthesis, structure, and biological effects of some bicyclic 5-isoxazolol zwitterions, J. Med. Chem. 29 (1986) 224–229.
[33] S. Imado, M. Shiro, Z. Horii, Structure of securinine hydrobromide dihydrate and the molecular structure of securinine, Chem. Pharm. Bull. 13 (1965) 643–651.
[34] T. Boulanger, D.P. Vercauteren, G. Evrard, F. Durant, Crystal structure and quantum electronic analysis of pitrazepin, a γ-amino-butyric acid (GABA) receptor antagonist, J. Chem. Soc., Perkin Trans. II (1989) 217–221.
[35] B.R. Brooks, R.E. Bruccoleri, B.D. Olafson, D.J. States, S. Swaminathan, M. Karplus, CHARMm: a program for macromolecular energy, minimization, and dynamics calculations, J. Comput. Chem. 4 (1983) 187–217.
[36] W.L. Jorgensen, Transferable intermolecular potential functions for water, alcohols, and ethers. Application to liquid water, J. Am. Chem. Soc. 103 (1981) 335–340.
[37] M.A. Simmonds, Classification of some GABA antagonists with regard to site of action and potency in slices of rat cuneate nucleus, Eur. J. Pharmacol. 80 (1982) 347–358.
[38] J.A. Beutler, E.W. Karbon, A.N. Brubacker, D. Malik, R. Curtis, S.J. Enna, Securinine alkaloids: a new class of GABA receptor antagonists, Brain Res. 330 (1985) 135–140.
[39] C.-G. Wermuth, J.-J. Bourguignon, G. Schlewer, J.-P. Gies, A. Schoenfelder, A. Melikian, M.-J. Bouchet, D. Chantreux, J.-C. Molimard, M. Heaulme, J.-P. Chambon, K. Biziere, Synthesis and structure–activity relationships of a series of aminopyridazine derivatives of γ-aminobutyric acid acting as selective $GABA_A$ antagonists, J. Med. Chem. 30 (1987) 239–249.
[40] B.H. Gähwiler, R. Maurer, K. Wüthrich, Pitrazepin, a novel $GABA_A$ antagonist, Neurosci. Lett. 45 (1984) 311–316.
[41] P. Krogsgaard-Larsen, L. Nielsen, E. Falch, D.R. Curtis, GABA agonists. Resolution, absolute stereochemistry, and enantioselectivity of (*S*)-(+)- and (*R*)-(−)-dyhydromuscimol, J. Med. Chem. 28 (1985) 1612–1617.
[42] R.D. Allan, H.W. Dickenson, J. Fong, Structure–activity studies on the activity of a series of cyclopentane GABA analogues on $GABA_A$ receptors and GABA uptake, Eur. J. Pharmacol. 122 (1986) 339–348.
[43] P. Krogsgaard-Larsen, E. Falch, H. Hjeds, Heterocyclic analogues of GABA: chemistry, molecular pharmacology and therapeutic aspects, Progr. Med. Chem. 22 (1985) 67–120.
[44] P. Krogsgaard-Larsen, GABA synaptic mechanisms: stereochemical and conformational requirements, Med. Res. Rev. 8 (1988) 27–56.